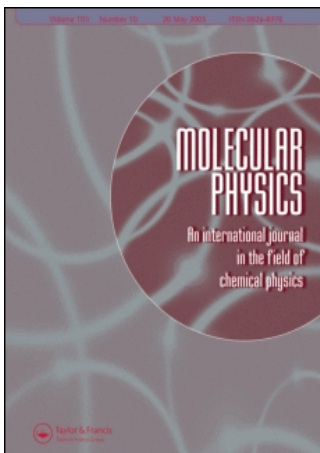


This article was downloaded by:[Canadian Research Knowledge Network]
On: 14 January 2008
Access Details: [subscription number 789349994]
Publisher: Taylor & Francis
Informa Ltd Registered in England and Wales Registered Number: 1072954
Registered office: Mortimer House, 37-41 Mortimer Street, London W1T 3JH, UK



Molecular Physics

An International Journal in the Field of Chemical Physics

Publication details, including instructions for authors and subscription information:
<http://www.informaworld.com/smpp/title~content=t713395160>

The formulation and implementation of analytic energy gradients for periodic density functional calculations with STO/NAO Bloch basis set

Eugene S. Kadantsev ^a; Rob Klooster ^b; Paul L. De Boeij ^b; Tom Ziegler ^a
^a Department of Chemistry, University of Calgary, Calgary, Alberta, T2N 1N4, Canada
^b Theoretical Chemistry, Zernike Institute for Advanced Materials, University of Groningen, Nijenborgh 4, 9747AG Groningen, The Netherlands

First Published on: 14 November 2007

To cite this Article: Kadantsev, Eugene S., Klooster, Rob, De Boeij, Paul L. and Ziegler, Tom (2007) 'The formulation and implementation of analytic energy gradients for periodic density functional calculations with STO/NAO Bloch basis set', Molecular Physics, 105:19, 2583 - 2596

To link to this article: DOI: 10.1080/00268970701598063

URL: <http://dx.doi.org/10.1080/00268970701598063>

PLEASE SCROLL DOWN FOR ARTICLE

Full terms and conditions of use: <http://www.informaworld.com/terms-and-conditions-of-access.pdf>

This article maybe used for research, teaching and private study purposes. Any substantial or systematic reproduction, re-distribution, re-selling, loan or sub-licensing, systematic supply or distribution in any form to anyone is expressly forbidden.

The publisher does not give any warranty express or implied or make any representation that the contents will be complete or accurate or up to date. The accuracy of any instructions, formulae and drug doses should be independently verified with primary sources. The publisher shall not be liable for any loss, actions, claims, proceedings, demand or costs or damages whatsoever or howsoever caused arising directly or indirectly in connection with or arising out of the use of this material.

The formulation and implementation of analytic energy gradients for periodic density functional calculations with STO/NAO Bloch basis set§

EUGENE S. KADANTSEV†, ROB KLOOSTER‡, PAUL L. DE BOEIJ‡ and TOM ZIEGLER*†

†Department of Chemistry, University of Calgary, Calgary, Alberta, T2N 1N4 Canada

‡Theoretical Chemistry, Zernike Institute for Advanced Materials, University of Groningen, Nijenborgh 4, 9747AG Groningen, The Netherlands

(Received 21 May 2007; in final form 25 July 2007)

Analytic energy gradients with respect to atomic coordinates for systems with translational invariance are formulated within the framework of Kohn–Sham Density Functional Theory. The energy gradients are implemented in the BAND program for periodic DFT calculations which directly employs a Bloch basis set made up of Slater-type (STOs) and numeric atomic orbitals (NAOs). The details of our implementation are described including the use of symmetry in the reciprocal and direct spaces, as well as the application of the frozen core approximation.

Keywords: Analytic gradients; Density Functional Theory; Periodic calculations; Bloch basis; Slater-type orbitals

1. Introduction

Over the past 30 years or so, the Kohn–Sham form of Density Functional Theory [1, 2] (KSDF) has become the method of choice for computational chemists and solid state physicists due to its very favourable compromise between the computational simplicity of the ‘noninteracting electron picture’ and the accuracy of methods in which electron correlation is taken into account. The conceptual advantage of DFT is that it is formally ‘exact’ in the limit of the exact exchange–correlation (xc) functional. It is hoped that further advances in the computational algorithms and improvements in the approximate xc models will make it possible to investigate systems composed of many thousand atoms from quantum mechanical first principles.

One of the early successes of DFT in chemistry was the formulation and implementation of analytic energy gradients for localized systems—molecules and clusters within the linear combination of atomic orbitals (LCAO) framework [3, 4] which was built upon some earlier attempts [5–9]. The DFT analytic gradients and

automatic schemes which employ these gradients were successfully applied to explore potential energy surfaces of molecules including the determination of the equilibrium molecular structures [3, 10] and transition states [11]. The analytic energy gradients are now routinely used to determine molecular energetics and are coded in all major DFT codes.

Note, however, that notwithstanding the famous Hellmann–Feynman theorem [12, 13], the derivation of the energy gradients with respect to nuclear displacements within the LCAO framework is not trivial for a finite LCAO basis. It was Peter Pulay [14] who showed that certain corrections to the Hellmann–Feynman force arise in the context of the LCAO framework and implemented analytic energy gradients for the Hartree–Fock (HF) wavefunction.

There is also a great interest in obtaining the analytic gradients for systems with translational invariance—polymers, surfaces, and crystals. Whereas the LCAO expansion is the ‘workhorse of computational chemistry’, the use of plane wave basis set is common in solid state physics [15]. In addition to being a ‘natural basis’

*Corresponding author. Email: ziegler@ucalgary.ca
§Paper is dedicated to Professor Peter Pulay.

for the three-dimensional periodic systems, the number and convergence of plane waves is controlled by a single parameter, the energy cut-off. Plane waves form an orthogonal basis set and do not depend explicitly on the atomic positions, therefore, the energy gradient is computed from the Hellmann–Feynman theorem and Pulay corrections are not required.

Unfortunately, the plane wave basis is not well suited for describing periodic systems with ‘defects’, for example, adsorbed molecules on the metal surface. In these cases, artificial supercells have to be introduced to impose periodicity in three-dimensions. In these supercells, physically relevant parts of the system are separated by large vacuum regions to avoid spurious interaction and many plane waves are wasted on describing the irrelevant vacuum. To put it in the words of Modine *et al.* [16], plane waves have infinite spatial extent and lack the important property of ‘adaptability’ or ‘localizability’ which is so important for implementation of the linear scaling techniques [17]. To achieve ‘localizability’, methods based, for example, on the real space grids have been proposed (for a review see [18]). A formulation in terms of the mixed plane-wave/LCAO approach [19] might also prove to be useful. The plane waves basis set is used in conjunction with first-principles pseudopotentials [20, 21] which have to be carefully tested on the subject of their transferability. While great progress has been made in developing transferable first-principles pseudopotentials [22, 23], the ultimate test of transferability of the pseudopotential is comparison to an accurate all-electron calculation.

Therefore, the LCAO expansion in the periodic calculations is deemed useful. Recently, a number of all-electron LCAO implementations of HF and KSDFT [24, 27] analytic energy gradients have been reported for systems with translational invariance. These implementations share several common features. Gaussian type atomic orbitals (GTOs) are employed. The KS(HF) Hamiltonian matrix elements are evaluated between the AOs and the lattice summations are performed to obtain the KS(HF) Hamiltonian matrix elements in the Bloch basis set. A regular grid in the reciprocal space is used. In the latter case, the \mathbf{P} -matrix in the AO basis set is related to the \mathbf{P} -matrix in the Bloch basis set by a simple Fourier transform.

A viable alternative to this AO approach to the periodic DFT calculations is to construct and use the Bloch basis set explicitly. This approach was systematically developed by te Velde and Baerends in the BAND program [28], a precise density functional

method for total energy calculation of systems with translational invariance. Due to the unique nature of BAND’s computational algorithms, none of the existing formulations of the analytical energy gradients are suitable for implementation in BAND.

In this paper, we report the implementation of the analytical energy gradient with respect to nuclear displacements in the BAND program. Our implementation differs from others in the explicit use of the Bloch basis set which is built from Slater-type atomic orbitals (STOs) and numerical atomic orbitals (NAOs). In principle, our implementation can utilize atomic orbitals of any type. The details of our implementation are described including the use of symmetry in the reciprocal and direct spaces as well as the frozen core approximation. The paper is organized in the following way. Section 2 briefly summarizes BAND’s unique computational scheme and presents a Pulay-type formula for the evaluation of analytic energy gradient for systems with translational invariance. The next several sections deal with the evaluation of individual contributions to the analytic gradient. This is followed by some applications and the concluding summary. Atomic units ($\hbar = m_e = e = a_0 = E_h = 1$) are used throughout.

2. BAND energy expression and energy gradient

The BAND program for periodic DFT calculations uses nonorthogonal Bloch basis set of the type

$$\chi_{\mu_A \mathbf{k}}(\mathbf{r}) = \sum_{\mathbf{T}} \exp\{\mathbf{i} \mathbf{k} \cdot \mathbf{T}\} \chi_{\mu_A}(\mathbf{r} - (\mathbf{R}_A + \mathbf{T})), \quad (1)$$

where each of the basis set functions $\chi_{\mu_A \mathbf{k}}$ is a linear combination of the ‘equivalent’ AOs (STOs or NAOs) centred on the sublattice of atoms A defined in the reference ($\mathbf{T} = 0$) Wigner–Seitz (WS) unit cell by vector \mathbf{R}_A and displaced with respect to the reference cell by a lattice vector \mathbf{T} . The Bloch basis set functions are evaluated on a grid of points inside the reference WS cell by lattice summations within the appropriate cut-off radius. The KS orbitals are then expanded in terms of N_V^B ‘valence’ basis set functions† (1)

$$\psi_{\mathbf{k}}^{\sigma}(\mathbf{r}) = \sum_A \sum_{\mu_A} c_{\mu_A}^{\sigma}(\mathbf{k}) \chi_{\mu_A \mathbf{k}}(\mathbf{r}), \quad \sigma = \alpha, \beta, \quad (2)$$

the KS Hamiltonian and the overlap matrices are set up, and the KS equations are solved with respect to the expansion coefficients $\{c_{\mu_A}^{\sigma}\}$. Since the KS Hamiltonian

† ‘Valence’ basis set function simply means that it describes electronic states which are treated variationally, as opposed to the ‘core’ functions which describe ‘frozen’ states.

depends on the electron density, this procedure is repeated until self-consistency is reached. Due to the underlying nature of the building blocks (STOs and NAOs) that make up $\chi_{\mu_A \mathbf{k}}$ in BAND, the analytic evaluation of the KS Hamiltonian matrix elements is impossible. Instead, the matrix elements are evaluated by a highly accurate Gaussian quadrature method [29, 30].

Basis set functions (1) are naturally ‘symmetrized’ with respect to the lattice translations $\hat{\mathbf{T}}$. A variable \mathbf{k} labels the *irreps* of the translational subgroup of the system’s space group. The resulting KS Hamiltonian is ‘block-diagonalized’ with respect to \mathbf{k} . In practice, this means that the computational cost for the calculations in the Bloch basis set is linear with respect to the number of \mathbf{k} points. Therefore, it is computationally expedient to make use of the symmetry in the reciprocal space† and restrict the possible values of \mathbf{k} to the symmetry unique wedge of the unit cell in the reciprocal space—the irreducible Brillouin zone (IBZ). The integration in the reciprocal space is required, for example, when the electron density is calculated during the SCF cycle.

In BAND, the BZ integration is carried out using the quadratic tetrahedron algorithm which works well for both metals and semiconductors [31, 32]. The electron density which has the full symmetry of the system (A1 symmetry) is obtained on the irreducible wedge of the WS cell (IWS) by performing the A1-projection:

$$\begin{aligned} \rho(\mathbf{r}) &= \sum_{\sigma=\alpha,\beta} \rho_{\sigma}(\mathbf{r}), \quad \rho_{\sigma}(\mathbf{r}) = \frac{1}{N_{\delta}} \sum_{\delta} \\ &\times \sum_{\sigma=\alpha,\beta} \rho_{\sigma}^{\text{irr}}(\{\mathbf{o}; \mathbf{t}_{\delta}\}^{-1}\mathbf{r}), \quad \mathbf{r} \in \text{IWS}, \\ \rho_{\sigma}^{\text{irr}}(\mathbf{r}) &= \sum_{\mathbf{k} \in \text{IBZ}} \sum_{AB} \sum_{\mu_A \nu_B} P_{\mu_A \nu_B}^{\sigma}(\mathbf{k}) \chi_{\mu_A \mathbf{k}}^{\dagger}(\mathbf{r}) \chi_{\nu_B \mathbf{k}}(\mathbf{r}), \quad \mathbf{r} \in \text{WS}, \\ P_{\mu_A \nu_B}^{\sigma}(\mathbf{k}) &= \sum_{\substack{\varepsilon_{\mathbf{k}}^{\sigma} < E_f}} n_i^{\sigma}(\mathbf{k}) c_{\mu_A i}^{\sigma \dagger}(\mathbf{k}) c_{\nu_B i}^{\sigma}(\mathbf{k}). \end{aligned} \quad (3)$$

The sum in (3) is over N_{δ} symmetry operations (generators)

$$\hat{\mathbf{o}}\mathbf{r} = \{\mathbf{o}; \mathbf{t}_{\delta}\}\mathbf{r} = \mathbf{o} \cdot \mathbf{r} + \mathbf{t}_{\delta} \quad (4)$$

consisting of the rigid rotation (point group part) \mathbf{o} followed by a nonprimitive translation \mathbf{t}_{δ} . The point group parts of the generators are symmetry operations

in the reciprocal space. The action of the operator $\hat{\mathbf{o}}^{-1}$ is defined as $\hat{\mathbf{o}}^{-1}\mathbf{r} = \{\mathbf{o}^{-1}; -\mathbf{o}^{-1}\mathbf{t}_{\delta}\}\mathbf{r} = \mathbf{o}^{-1} \cdot (\mathbf{r} - \mathbf{t}_{\delta})$. The elements of the so-called \mathbf{P}^{σ} -matrix in (3) are obtained by summing over all energy bands which are below the Fermi energy E_f ; $n_i^{\sigma}(\mathbf{k}) = \tilde{n}_i^{\sigma}(\mathbf{k})w(\mathbf{k})$ are ‘generalized’ occupation numbers corresponding to the *i*th band—occupation numbers $\tilde{n}_i^{\sigma}(\mathbf{k})$ weighted for the IBZ integration by the factor $w(\mathbf{k})$ according to [31, 32]. It is also expedient to introduce the spin-traced \mathbf{P} -matrix with elements $P_{\mu_A \nu_B}(\mathbf{k}) = P_{\mu_A \nu_B}^{\alpha}(\mathbf{k}) + P_{\mu_A \nu_B}^{\beta}(\mathbf{k})$.

The total energy per unit cell $E = T_s + E_{\text{xc}} + E_{\text{Coul}}$ is a sum of the kinetic, xc, and the Coulomb contributions, respectively, where

$$\begin{aligned} T_s[\rho] &= \sum_{\mathbf{k} \in \text{IBZ}} \sum_{AB} \sum_{\mu_A \nu_B} P_{\mu_A \nu_B}(\mathbf{k}) \langle \chi_{\mu_A \mathbf{k}} | -\frac{1}{2} \nabla^2 | \chi_{\nu_B \mathbf{k}} \rangle, \\ E_{\text{xc}}[\rho_{\alpha}, \rho_{\beta}] &= \int_{\text{WS}} F_{\text{xc}}(\rho_{\alpha}, \rho_{\beta}, \nabla \rho_{\alpha}, \nabla \rho_{\beta}) \, \mathbf{d}\mathbf{r}, \\ E_{\text{Coul}}[\rho] &= \frac{1}{2} \sum_{A,B} \sum_{\mathbf{T}} \int \rho_0^A(r_A) V_{\mathbf{T}}^B(r_B) \, \mathbf{d}\mathbf{r} \\ &+ \sum_B \int_{\text{WS}} \Delta \rho(\mathbf{r}) V^B \, \mathbf{d}\mathbf{r} \\ &+ \frac{1}{2} \int_{\text{WS}} \Delta \rho(\mathbf{r}) \Delta V(\mathbf{r}) \, \mathbf{d}\mathbf{r} + \sum_A E_{\text{Coul}}^A, \\ \Delta \rho(\mathbf{r}) &= \rho(\mathbf{r}) - \sum_C \rho_e^C, \quad \rho_e^C = \sum_{\mathbf{T}} \rho_{\mathbf{T},e}^C(r_C), \\ V^B &= \sum_{\mathbf{T}} V_{\mathbf{T}}^B(r_B), \\ \rho_{\mathbf{T},e}^C(r_C) &= \rho_e^C(|\mathbf{r} - \mathbf{R}_C - \mathbf{T}|), \\ \rho_{\mathbf{T}}^B(r_B) &= \rho_{\mathbf{T},e}^B(r_B) - Z_B \delta(\mathbf{r} - \mathbf{R}_B - \mathbf{T}). \end{aligned} \quad (5)$$

In (5), $F_{\text{xc}}(\rho_{\alpha}, \rho_{\beta}, \nabla \rho_{\alpha}, \nabla \rho_{\beta})$ is some ‘local’ function of the electron density and possibly density gradient which encompasses the local density (LDA) and generalized gradient approximations (GGA) [33] for the xc energy. The first term in the Coulomb contribution is referred to as the *PAIR* term. The *PAIR* term, describes electrostatic ‘pair’ interactions between two neutral spherically symmetric charge distributions located at the atomic site \mathbf{R}_A in cell $\mathbf{T}=0$ and at the site \mathbf{R}_B in the cell labelled by \mathbf{T} . The subscript *e* in $\rho_{\mathbf{T},e}^B$ denotes the electronic part of the atomic density. $V_{\mathbf{T}}^B(r_B)$ and V^B denote electrostatic atomic potential corresponding to a neutral spherically symmetric charge distribution $\rho_{\mathbf{T}}^B(r_B)$ and its lattice sum, respectively. All the electrostatic potentials correspond to the charge neutral objects and the corresponding lattice sums converge rapidly. The prime at the sum

† Apart from the time-reversal symmetry, the symmetry in the reciprocal space stems from the symmetry in the direct space, it has no symmetry of its own.

sign in the *PAIR* term means that the atomic self-interaction is omitted in $\mathbf{T}=0$. The charge neutral and A1-symmetric electron deformation density $\Delta\rho(\mathbf{r})$ is the difference between the electron SCF density $\rho(\mathbf{r})$ (3) and the sum of the atomic electron densities. ΔV denotes the electrostatic potential which corresponds to $\Delta\rho(\mathbf{r})$ and which is obtained via a global fit under the constraint that the fitted deformation density integrates to zero [34]. Finally, the last term in the Coulomb energy is a sum of Coulomb atomic energies E_{Coul}^A (see [30] p. 58)†. As explained below, this term will not contribute to the energy gradient as the sum of ‘one-centre’ contributions and can be omitted from further consideration. Note also that all terms in (5) can be evaluated from the IBZ information only.

The derivation of the gradients in the periodic case follows that of molecules. The main distinction is that we have to perform integration in the reciprocal space and that the electrostatic terms should be properly combined. Assuming that self-consistency is reached, after some algebra we obtain a Pulay-type formula for the density functional energy gradient with respect to the Cartesian coordinate γ of an atom C located at \mathbf{R}_C

$$\begin{aligned} \frac{dE}{dR_C^\gamma} &= - \sum_{\mathbf{k} \in \text{BZ}} \sum_{AB} \sum_{\mu_A \nu_B} P_{\mu_A \nu_B}^e(\mathbf{k}) \frac{\partial S_{\mu_A \nu_B}(\mathbf{k})}{\partial R_C^\gamma} + \frac{\partial T_s}{\partial R_C^\gamma} \\ &\quad + \sum_{\sigma=\alpha,\beta} \int V_{\text{xc}}^\sigma(\mathbf{r}) \frac{\partial \rho^\sigma(\mathbf{r})}{\partial R_C^\gamma} d\mathbf{r} + \frac{\partial E_{\text{Coul}}}{\partial R_C^\gamma}, \\ P_{\mu_A \nu_B}^e(\mathbf{k}) &= \sum_{\sigma=\alpha,\beta} P_{\mu_A \nu_B}^{e\sigma}(\mathbf{k}), \\ P_{\mu_A \nu_B}^{e\sigma}(\mathbf{k}) &= \sum_{\varepsilon_{\mathbf{k}}^\sigma < E_f} n_i^\sigma(\mathbf{k}) \varepsilon_i^\sigma(\mathbf{k}) c_{\mu_A i}^{\sigma\dagger}(\mathbf{k}) c_{\nu_B i}^\sigma(\mathbf{k}). \end{aligned} \quad (6)$$

The first term in (6) stems from the explicit dependence of the LCAO energy expression on the \mathbf{P} -matrix elements which, in turn, implicitly depend on the nuclear coordinates through the SCF solution. This term involves the eigenvalue- or energy-weighted \mathbf{P}^e -matrix and derivatives of the overlap matrix elements $S_{\mu_A \nu_B}(\mathbf{k}) = \langle \chi_{\mu_A \mathbf{k}} | \chi_{\nu_B \mathbf{k}} \rangle$. The second, third, and fourth terms are explicit partial derivatives of the kinetic, xc, and the Coulomb electrostatic energy, respectively. The xc contribution involves the xc-potential defined as $V_{\text{xc}}^\sigma(\mathbf{r}) = \delta E_{\text{xc}}[\rho_\alpha, \rho_\beta] / \delta \rho_\sigma(\mathbf{r})$. The potential V_{xc}^σ is always evaluated in BAND explicitly. In the case of the kinetic energy and xc-energy contributions to the analytic gradient, the explicit dependence on the nuclear

coordinates is entirely due to the LCAO nature of the basis set. In the case of the electrostatic energy contribution, the explicit dependence stems from the LCAO basis set as well as from the external atomic potential. The Hellmann–Feynmann force is ‘buried’ in the last electrostatic contribution.

The following is relevant when implementing gradients in BAND.

- (i) BAND energy relies on a numerical integration scheme to evaluate integrals which involve Bloch basis set functions. It is expected that numerical evaluation of integrals that involve gradients of the basis set functions is more challenging. Therefore, it is important to make sure that the numerical errors are minimized.
- (ii) The energy gradient (6) involves integration in the reciprocal space over the whole BZ. We have to employ symmetry in the reciprocal space to compute the energy gradient from IBZ, and, therefore, we will need to know how to transform Bloch basis set functions and their gradients in the symmetry related \mathbf{k} -points.
- (iii) For efficient implementation of the gradients, we will also make use of symmetry in the direct space. To reduce the number of electrons which have to be treated variationally, it is expedient to implement gradient within the frozen core approximation (FCA) [35, 36].

With respect to the accuracy considerations we note that certain terms that contribute to the total energy will not contribute to the energy gradient. These terms should be removed from the energy expression *a priori* to avoid ‘numerical noise’. One important example of such terms are the one-centre terms—the energy contributions which depend solely on one ‘sublattice’. A one-centre energy contribution can be, for example, an overlap integral (or a kinetic energy integral) between two Bloch functions which are built from the AOs belonging to the same sublattice. It is clear that by moving an atom in the reference cell and, moving all its ‘translational’ copies in the other cells we do not change the integral’s value. Therefore, a partial derivative of the one-centre terms with respect to any atomic coordinate is always analytically zero. The same can be said about the electrostatic contributions to the energy which depend only on one sublattice—these terms will not contribute to any partial derivatives (with respect to the atomic coordinates).

†BAND’s Coulomb energies and lattice summations are extensively discussed in te Velde’s PhD thesis which can be freely downloaded from www.scm.com

The first energy derivatives with respect to the atomic coordinates can be evaluated from the IBZ based on the symmetry transformation properties of the Bloch basis set functions. As shown in the Appendix A, the expectation value of an operator \hat{A} can be computed from IBZ as

$$\begin{aligned} & \frac{1}{N_{\hat{o}}} \sum_{\hat{o}} \sum_{\mathbf{k} \in \text{IBZ}} \sum_{AB} \sum_{\mu_A \nu_B} P_{\mu_A \nu_B}(\mathbf{ok}) \langle \chi_{\mu_A \mathbf{ok}} | \hat{A} | \chi_{\nu_B \mathbf{ok}} \rangle \\ &= \frac{1}{N_{\hat{o}}} \sum_{\hat{o}} \sum_{\mathbf{k} \in \text{IBZ}} \sum_{AB} \sum_{\mu_A \nu_B} P_{\mu_A \nu_B}(\mathbf{k}) \langle \{\mathbf{o}; \mathbf{t}_o\} \chi_{\mu_A \mathbf{k}} | \hat{A} | \{\mathbf{o}; \mathbf{t}_o\} \chi_{\nu_B \mathbf{k}} \rangle, \end{aligned} \quad (7)$$

where $\{\mathbf{o}; \mathbf{t}_o\} \chi_{\mu_A \mathbf{k}}$ and $\{\mathbf{o}; \mathbf{t}_o\} \chi_{\nu_B \mathbf{k}}$ are Bloch basis set functions rotated in the real space

$$\begin{aligned} & \{\mathbf{o}; \mathbf{t}_o\} \chi_{\mu_A \mathbf{k}}(\mathbf{r}) \\ &= \sum_{\mathbf{T}} \exp \{i \mathbf{k} \mathbf{T}\} \chi_{\mu_A}(\mathbf{o}^{-1}(\mathbf{r} - \mathbf{R}_{(\hat{o}A)} - \mathbf{T}_A(\mathbf{o}) - \mathbf{o} \mathbf{T})). \end{aligned} \quad (8)$$

Note that the symmetry operation \hat{o} transforms an AO centred on atom A into the rotated AO centred on the symmetry related atom ($\hat{o}A$) with coordinate $\mathbf{R}_{(\hat{o}A)} + \mathbf{T}_A(\mathbf{o}) = \mathbf{o} \mathbf{R}_A + \mathbf{t}_o$. The symmetry operations always map one sublattice of atoms into another apart from, perhaps, a primitive lattice vector ($\mathbf{T}_A(\mathbf{o})$) [37]. From (8) it follows that the gradient of the rotated Bloch function transforms as

$$\left(\frac{\partial \{\mathbf{o}; \mathbf{t}_o\} \chi_{\mu_A \mathbf{k}}}{\partial r^\gamma} \right) \Big|_{\mathbf{r}} = \sum_{\alpha=1}^3 (\mathbf{o})_{\gamma\alpha} \left(\frac{\partial \chi_{\mu_A \mathbf{k}}}{\partial r^\alpha} \right) \Big|_{\hat{o}^{-1} \mathbf{r}}. \quad (9)$$

Finally, it is expedient to use the symmetry in the direct space to perform the numerical integration of the terms involving the gradient of electron density—the xc contribution and the Coloumb contribution. The use of the symmetry in the direct space is described in section 5 which deals with the xc and electrostatic contributions. It suffices to say here that electron density gradients with respect to atomic coordinates can be evaluated on IWS only.

The rest of the paper is organized as follows. Section 3 describes evaluation of the kinetic energy and the energy-weighted \mathbf{P} -matrix contributions to the analytic gradients. Section 4 describes the computation of the electron density gradient which enters the expressions for the xc-energy and Coulomb contributions. Section 5 deals with evaluation of the Coulomb and xc-energy contributions. This is followed by a brief discussion of the frozen core approximation and numerical examples.

3. Kinetic energy contribution and energy-weighted \mathbf{P} -matrix contribution to analytic gradient

In this section, we consider contributions from the kinetic energy and energy-weighted \mathbf{P}^e -matrix to the analytic gradient. ‘Physically’, the two terms have a different origin. The energy-weighted \mathbf{P}^e -matrix contribution stems from the explicit dependence of the energy on the MO coefficients and orthogonality constraints, whereas the kinetic energy contribution $\partial T_s / \partial R_C^\gamma$ stems from the explicit dependence of the basis set functions on the atomic coordinates. In practice, evaluation of both terms is very similar.

Let us consider the kinetic energy contribution in detail, as it is a little bit more complicated. Using (7), the kinetic energy writes as

$$\begin{aligned} T_s &= \frac{1}{N_{\hat{o}}} \sum_{\hat{o}} \sum_{\mathbf{k} \in \text{IBZ}} \sum_{AB} \sum_{\mu_A \nu_B} T_{\mu_A \nu_B}(\mathbf{ok}), \\ T_{\mu_A \nu_B}(\mathbf{ok}) &= \text{Re} \left\{ \bar{P}_{\mu_A \nu_B}(\mathbf{k}) \langle \{\mathbf{o}; \mathbf{t}_o\} \chi_{\mu_A \mathbf{k}} | -\frac{1}{2} \nabla^2 | \{\mathbf{o}; \mathbf{t}_o\} \chi_{\nu_B \mathbf{k}} \rangle \right\}, \end{aligned} \quad (10)$$

where $\bar{P}_{\mu_A \nu_B}(\mathbf{k}) = 2P_{\mu_A \nu_B}(\mathbf{k})$ for $\mu_A \neq \nu_B$ and $\bar{P}_{\mu_A \mu_A}(\mathbf{k}) = P_{\mu_A \mu_A}(\mathbf{k})$. The sum (10) is over $N_v^B * (N_v^B - 1)/2$ distinct $\{\mu_A, \nu_B\}$ pairs. The diagonal terms $\{A, \mu_A\} = \{B, \nu_B\}$ *a priori* will not contribute to the gradient as these are one-centre terms and can be excluded. For each ‘pair’ $\{A, \mu_A\}, \{B, \nu_B\}$ we then analyse assignment of $\chi_{\mu_A \mathbf{k}}$ and $\chi_{\nu_B \mathbf{k}}$ Bloch functions and omit the term from consideration if both basis functions are centred on the same sublattice ($A = B$). If $\{\mathbf{o}; \mathbf{t}_o\}$ is the identity operator, each of the remaining two-centre terms will then contribute to the derivatives with respect to R_A^γ and R_B^γ

$$\begin{aligned} \frac{\partial T_{\mu_A \nu_B}(\mathbf{k})}{\partial R_A^\gamma} &= -\text{Re} \left\{ \bar{P}_{\mu_A \nu_B}(\mathbf{k}) \left\langle \frac{\partial \chi_{\mu_A \mathbf{k}}}{\partial r^\gamma} \middle| -\frac{1}{2} \nabla^2 | \chi_{\nu_B \mathbf{k}} \right\rangle \right\}, \\ \frac{\partial T_{\mu_A \nu_B}(\mathbf{k})}{\partial R_B^\gamma} &= -\text{Re} \left\{ \bar{P}_{\mu_A \nu_B}(\mathbf{k}) \left\langle \frac{\partial \chi_{\mu_A \mathbf{k}}}{\partial r^\gamma} \middle| -\frac{1}{2} \nabla^2 | \chi_{\nu_B \mathbf{k}} \right\rangle^\dagger \right\}, \end{aligned} \quad (11)$$

respectively, where $\gamma = \{x, y, z\}$ or $\gamma = \{1, 2, 3\}$. Note that in the second equation of (11) we used complex conjugation to avoid differentiation of the Laplacian of the basis set functions.

In the symmetry related \mathbf{k} -point— \mathbf{ok} , we obtain

$$\begin{aligned} \nabla_{\mathbf{R}_{(\hat{o}A)}} T_{\mu_A \nu_B}(\mathbf{ok}) &= -\mathbf{o} \cdot \text{Re} \left\{ \bar{P}_{\mu_A \nu_B}(\mathbf{k}) \langle \nabla \chi_{\mu_A \mathbf{k}} | -\frac{1}{2} \nabla^2 | \chi_{\nu_B \mathbf{k}} \rangle \right\}, \\ \nabla_{\mathbf{R}_{(\hat{o}B)}} T_{\mu_A \nu_B}(\mathbf{ok}) &= -\mathbf{o} \cdot \text{Re} \left\{ \bar{P}_{\mu_A \nu_B}(\mathbf{k}) \langle \nabla \chi_{\nu_B \mathbf{k}} | -\frac{1}{2} \nabla^2 | \chi_{\mu_A \mathbf{k}} \rangle^\dagger \right\}, \end{aligned} \quad (12)$$

where we used (9) for the gradient of the rotated basis set function. In (12), $\nabla_{\mathbf{R}(\hat{o}A)}$ and $\nabla_{\mathbf{R}(\hat{o}B)}$ denote a three-component gradient with respect to coordinates of atoms ($\hat{o}A$) and ($\hat{o}B$), respectively. The final expression for the gradient of the kinetic energy writes

$$\begin{aligned} \frac{\partial T_s}{\partial R_C^\gamma} = & -\frac{1}{N_{\hat{o}}} \sum_{\hat{o}} \sum_{\mathbf{k} \in \text{IBZ}} \sum_{A \neq B} \sum_{\mu_A \nu_B} \\ & \times \text{Re} \left\{ \bar{P}_{\mu_A \nu_B}(\mathbf{k}) \sum_{\alpha} (\mathbf{o})_{\gamma\alpha} \left[\delta_{C(\hat{o}A)} \left\langle \frac{\partial \chi_{\mu_A \mathbf{k}}}{\partial r^\alpha} \right| -\frac{1}{2} \nabla^2 | \chi_{\nu_B \mathbf{k}} \right\rangle \right. \\ & \left. + \delta_{C(\hat{o}B)} \left\langle \frac{\partial \chi_{\nu_B \mathbf{k}}}{\partial r^\alpha} \right| -\frac{1}{2} \nabla^2 | \chi_{\mu_A \mathbf{k}} \rangle^\dagger \right] \right\}. \end{aligned} \quad (13)$$

In practice, we compute all the gradients in the IBZ via equation (11) and then, in the end, perform ‘symmetrization’ of the gradients by ‘averaging’ over the symmetry operations using (12).

The algorithm for calculation of the energy-weighted \mathbf{P} -matrix contribution to the analytic gradient follows closely the calculation of the kinetic energy contribution. We again analyse only those $\{\mu_A, \nu_B\}$ pairs for which the basis set functions are assigned to different sublattices $A \neq B$. The resulting equations follow closely (11), (12) and (13) if we replace ∇^2 by the identity operator and replace the \mathbf{P} -matrix by \mathbf{P}^e -matrix (6). The final expression is given by

$$\begin{aligned} \frac{1}{N_{\hat{o}}} \sum_{\hat{o}} \sum_{\mathbf{k} \in \text{IBZ}} \sum_{A \neq B} \sum_{\mu_A \nu_B} \text{Re} \left\{ \bar{P}_{\mu_A \nu_B}^e(\mathbf{k}) \sum_{\alpha} (\mathbf{o})_{\gamma\alpha} \right. \\ \left. \times \left[\delta_{C(\hat{o}A)} \left\langle \frac{\partial \chi_{\mu_A \mathbf{k}}}{\partial r^\alpha} \right| \chi_{\nu_B \mathbf{k}} \right\rangle + \delta_{C(\hat{o}B)} \left\langle \chi_{\mu_A \mathbf{k}} \right| \frac{\partial \chi_{\nu_B \mathbf{k}}}{\partial r^\alpha} \right] \right\}. \end{aligned} \quad (14)$$

Finally, we note that the linear scaling techniques are used to speed up numerical integration. The whole simulation region is partitioned into blocks and the integration is performed on the block by block basis. Only the basis functions which are not identically zero are considered for the integration in the given block. In practice, this means that for each block we consider only a subset of the basis set functions in (10).

4. Gradient of the electron density

Gradient of the electron density with respect to the atomic coordinates is required for calculation of the xc and Coulomb terms in (6). This gradient is precalculated for each atomic coordinate on the IWS and stored on the disk from which it can be later retrieved.

The calculation of the density gradient proceeds in the following way. According to (7), the electron density can be computed from the IBZ as

$$\begin{aligned} \rho_\sigma(\mathbf{r}) = & \frac{1}{N_{\hat{o}}} \sum_{\hat{o}} \sum_{\mathbf{k} \in \text{IBZ}} \sum_{AB} \sum_{\mu_A \nu_B} \rho_{\mu_A \nu_B, \sigma}(\mathbf{o}\mathbf{k}, \mathbf{r}), \\ \rho_{\mu_A \nu_B, \sigma}(\mathbf{o}\mathbf{k}, \mathbf{r}) = & \text{Re} \left\{ \bar{P}_{\mu_A \nu_B}^\sigma(\mathbf{k}) (\{\mathbf{o}; \mathbf{t}_o\} \chi_{\mu_A \mathbf{k}}(\mathbf{r}))^\dagger (\{\mathbf{o}; \mathbf{t}_o\} \chi_{\nu_B \mathbf{k}}(\mathbf{r})) \right\}, \end{aligned} \quad (15)$$

where we loop over $N_V^B(N_V^B + 1)/2$ pairs of Bloch basis set functions and \bar{P} -matrix is defined through the \mathbf{P} -matrix as in section 3. Note that the one-centre contributions should not be removed from the density. Next, we consider a fixed $\{\mu_A, \nu_B\}$ ‘pair’ density $\rho_{\mu_A \nu_B, \sigma}(\mathbf{k}, \mathbf{r})$ at \mathbf{k} -point in the IBZ. The derivative of this ‘pair’ density is

$$\begin{aligned} \frac{\partial \rho_{\mu_A \nu_B, \sigma}(\mathbf{k}, \mathbf{r})}{\partial R_A^\gamma} = & -\text{Re} \left\{ \bar{P}_{\mu_A \nu_B}^\sigma(\mathbf{k}) \frac{\partial \chi_{\mu_A \mathbf{k}}^\dagger(\mathbf{r})}{\partial r^\gamma} \chi_{\nu_B \mathbf{k}}(\mathbf{r}) \right\}, \quad \mathbf{r} \in \text{WS}, \\ \frac{\partial \rho_{\mu_A \nu_B, \sigma}(\mathbf{k}, \mathbf{r})}{\partial R_B^\gamma} = & -\text{Re} \left\{ \bar{P}_{\mu_A \nu_B}^\sigma(\mathbf{k}) \chi_{\mu_A \mathbf{k}}^\dagger(\mathbf{r}) \frac{\partial \chi_{\nu_B \mathbf{k}}(\mathbf{r})}{\partial r^\gamma} \right\}, \quad \mathbf{r} \in \text{WS}. \end{aligned} \quad (16)$$

In the symmetry related \mathbf{k} -point outside of the IBZ— $\mathbf{o}\mathbf{k}$, the contributions to the gradient stem from the rotated ‘pair’ density $\rho_{\mu_A \nu_B, \sigma}(\mathbf{o}\mathbf{k}, \mathbf{r})$. Taking into account (9), we can express gradient of the rotated ‘pair’ density in terms of the gradient (16)

$$\nabla_{\mathbf{R}(\hat{o}A)} \rho_{\mu_A \nu_B, \sigma}(\mathbf{o}\mathbf{k}, \mathbf{r}) = \mathbf{o} \cdot \nabla_{R_A} \rho_{\mu_A \nu_B, \sigma}(\mathbf{k}, \hat{o}^{-1}\mathbf{r}), \quad (17)$$

where the vector notation introduced in section 3 is used. The final expression for the density gradient is given by

$$\begin{aligned} \frac{\partial \rho(\mathbf{r})}{\partial R_C^\gamma} = & -\frac{1}{N_{\hat{o}}} \sum_{\hat{o}} \sum_{\mathbf{k} \in \text{IBZ}} \sum_{AB} \sum_{\mu_A \nu_B} \text{Re} \left\{ \bar{P}_{\mu_A \nu_B}(\mathbf{k}) \sum_{\alpha} (\mathbf{o})_{\gamma\alpha} \right. \\ & \left. \times \left[\delta_{C(\hat{o}A)} \frac{\partial \chi_{\mu_A \mathbf{k}}}{\partial r^\alpha} \chi_{\nu_B \mathbf{k}} + \delta_{C(\hat{o}B)} \chi_{\mu_A \mathbf{k}} \frac{\partial \chi_{\nu_B \mathbf{k}}}{\partial r^\alpha} \right] \Big|_{\hat{o}^{-1}\mathbf{r}} \right\}. \end{aligned} \quad (18)$$

As in the case of the kinetic energy contribution, the gradients are computed on the IBZ using (16) which is followed by symmetrization (17).

5. Coulomb energy contribution and xc-energy contribution to analytic gradient

Both, Coulomb and xc-energy terms in (6) involve density gradient. Most of the electrostatic energy comes

from the so-called *PAIR* term. The *PAIR* term is at least one magnitude larger than the electrostatic terms involving the deformation density $\Delta\rho(\mathbf{r})$. We will refer to these ‘smaller’ electrostatic terms as the ‘non-pair’ terms. The evaluation of the gradient of the non-pair electrostatic terms is very similar to the evaluation of the xc-energy contribution to the analytic gradient.

Differentiating the electrostatic contribution (sum of atomic Coulomb energies is omitted) to the energy of the crystal per WS cell we obtain

$$\begin{aligned} \frac{\partial E_{\text{Coul}}}{\partial R_B^\gamma} &= \frac{\partial PAIR}{\partial R_B^\gamma} + \int_{\text{WS}} \frac{\partial \Delta\rho}{\partial R_B^\gamma} \left(\sum_C V^C \right) d\mathbf{r} \\ &\quad + \int_{\text{WS}} \Delta\rho \frac{\partial V^B}{\partial R_B^\gamma} d\mathbf{r} + \int_{\text{WS}} \frac{\partial \Delta\rho}{\partial R_B^\gamma} \Delta V d\mathbf{r} \\ &= \frac{\partial PAIR}{\partial R_B^\gamma} + \int_{\text{WS}} \frac{\partial \Delta\rho}{\partial R_B^\gamma} V_{\text{Coul}} d\mathbf{r} + \int_{\text{WS}} \frac{\partial \Delta\rho}{\partial r^\gamma} V^B d\mathbf{r}, \\ V_{\text{Coul}}(\mathbf{r}) &= \left(\sum_C V^C + \Delta V \right), \end{aligned} \quad (19)$$

where we used integration by parts

$$\int_{\text{WS}} \Delta\rho \frac{\partial V^B}{\partial R_B^\gamma} d\mathbf{r} = - \int_{\text{WS}} \Delta\rho \frac{\partial V^B}{\partial r^\gamma} d\mathbf{r} = \int_{\text{WS}} \frac{\partial \Delta\rho}{\partial r^\gamma} V^B d\mathbf{r}. \quad (20)$$

It is of paramount importance that the derivative of the pair term is evaluated as accurately as possible. Fortunately, evaluation of $\partial PAIR / \partial R_B^\gamma$ is possible with almost any precision using a special coordinate transformation as described in section 5.2. The electrostatic non-pair terms in (19) have to be evaluated using three-dimensional numerical integration. The second and the third terms in (19) involve derivatives of the deformation density

$$\frac{\partial \Delta\rho}{\partial R_B^\gamma} = \frac{\partial \rho}{\partial R_B^\gamma} - \frac{\partial \rho_e^B}{\partial R_B^\gamma} \quad (21)$$

and

$$\frac{\partial \Delta\rho}{\partial r^\gamma} = - \sum_C \frac{\partial \Delta\rho}{\partial R_C^\gamma}. \quad (22)$$

The non-pair terms in (19) involve also the total electrostatic and electrostatic atomic potentials V_{Coul} and V^B .

Note that these non-pair terms contain

$$\frac{\partial \Delta\rho^B}{\partial R_B^\alpha} V^B - \frac{\partial \Delta\rho^B}{\partial R_B^\alpha} V^B, \quad (23)$$

which leads to the exact cancellation of the one-centre terms of the type

$$\frac{\partial \Delta\rho^B}{\partial R_B^\alpha} V^B. \quad (24)$$

The only remaining ‘one-centre’ terms are of the form

$$\int_{\text{WS}} \frac{\partial \Delta\rho^B}{\partial R_B^\alpha} \Delta V^B d\mathbf{r}. \quad (25)$$

It is expected that these smaller terms can be handled by BAND’s three-dimensional integrational scheme with sufficient accuracy.

The gradient of the Coulomb energy is calculated using equation (19) from the SCF density gradient (18). The evaluation of the *PAIR* term is described in section 5.2., whereas the next section describes evaluation of terms which involve density gradient from the IWS.

5.1. XC contribution to the analytic gradient: IWS integration

The density gradient can be computed only on the IWS and the symmetry in the direct space can be used to calculate certain integrals over the whole WS. Let us demonstrate this by evaluating the xc-energy contribution to the analytic gradient. Note that from the computational point of view, the evaluation of the xc contribution is identical to the evaluation of the non-pair electrostatic term which involves the total Coulomb potential—both terms contain a product of A1-symmetric potentials (V_{Coul} and V_{xc}^σ) and a density gradient. The integral over the WS can be written as

$$\begin{aligned} \frac{\partial E_{\text{xc}}}{\partial R_B^\gamma} &= \sum_\sigma \int_{\text{WS}} \frac{\partial \rho_\sigma(\mathbf{r})}{\partial R_B^\gamma} V_{\text{xc}}^\sigma(\mathbf{r}) d\mathbf{r} = - \sum_\sigma \sum_{\hat{o}} I^\sigma(\hat{o}), \\ I^\sigma(\hat{o}) &= \int_{\hat{o}(\text{IWS})} \frac{\partial \tilde{\rho}_\sigma^B(\mathbf{r})}{\partial r^\gamma} V_{\text{xc}}^\sigma(\mathbf{r}) d\mathbf{r}, \end{aligned} \quad (26)$$

where $\tilde{\rho}_\sigma^B(\mathbf{r})$ is a part of the SCF density which explicitly depends on atom B (see Appendix B). We now consider integral $I^\sigma(\hat{o})$ and coordinate transformation $\mathbf{r}' = \hat{o}^{-1}\mathbf{r}$ which maps $\hat{o}(\text{IWS}) \rightarrow \text{IWS}$. Due to the A1-symmetry, $V_{\text{xc}}^\sigma(\mathbf{r}') = V_{\text{xc}}^\sigma(\mathbf{r})$; the volume element $d\mathbf{r}$ remains unchanged; it is shown in Appendix B (equation (B9)) that $\tilde{\rho}_\sigma^B(\mathbf{r})$ transforms as $\tilde{\rho}_\sigma^B(\hat{o}\mathbf{r}') = \tilde{\rho}_\sigma^{\hat{o}^{-1}B}(\mathbf{r}')$ and

$$\frac{\partial}{\partial r^\gamma} = \sum_{\alpha=1}^3 \frac{\partial}{\partial r'^\alpha} \frac{\partial r'^\alpha}{\partial r^\gamma} = \sum_{\alpha=1}^3 \frac{\partial}{\partial r'^\alpha} (\mathbf{o})_{\gamma\alpha}. \quad (27)$$

After carrying out the change of variables in the integral, we obtain an expression for the xc contribution to the analytic gradient which involves only integration of quantities defined on the IWS

$$\frac{\partial E_{xc}}{\partial R_{(\hat{\alpha}B)}^\gamma} = \sum_{\sigma} \sum_{\hat{\alpha}} \sum_{\alpha=1}^3 (\mathbf{o})_{\gamma\alpha} \int_{IWS} \frac{\partial \rho_{\sigma}(\mathbf{r})}{\partial R_B^{\alpha}} V_{xc}^{\sigma}(\mathbf{r}) d\mathbf{r}. \quad (28)$$

It is shown in Appendix B that the spherically symmetric atomic density transforms the same way as the atom-dependent chunk of the SCF density and, therefore, we can replace $V_{xc}^{\sigma}(\mathbf{r}) \rightarrow V_{Coul}(\mathbf{r})$ and $\rho(r) \rightarrow \Delta\rho(r)$ to obtain the expression for the calculation of the first part of the non-pair Coulomb contribution from the IWS (19). Reduction of integral (20) can be accomplished along similar lines.

5.2. Derivative of the pair electrostatic energy

The first term in (19) $\partial PAIR/\partial R_B^{\alpha}$ can be evaluated in polar spheroidal coordinates with almost arbitrary precision. Each pair of atoms ($A(\mathbf{T}), B$), $A \neq B$ in the pair interaction will contribute only to derivatives $\partial/\partial R_A^{\alpha}$ and $\partial/\partial R_B^{\alpha}$. Note that the pair interaction between two atoms that belong to the same (two identical atoms separated by a lattice vector \mathbf{T}) will not contribute to the energy derivative $\partial/\partial R_A^{\alpha}$ since it is a ‘one-centre’ integral. Therefore, a simple strategy for calculation of the *PAIR* derivative is to run over all pairs of atoms ($A(\mathbf{T}), B$), $A \neq B$ within a certain cut-off distance from the reference WS cell and calculate each pair contribution to $\partial/\partial R_A^{\alpha}$ and $\partial/\partial R_B^{\alpha}$.

Differentiation of each pair can be accomplished in the following way. Consider a two-centre integral

$$I(\mathbf{R}_A, \mathbf{R}_B, \mathbf{T}) = I(d) = \int \rho^A(|\mathbf{r}|) V^B(|\mathbf{r} - \mathbf{d}|) d\mathbf{r}, \quad (29)$$

where $\mathbf{d} = \mathbf{R}_B + \mathbf{T} - \mathbf{R}_A$ and $d = |\mathbf{d}|$ is the distance between the two centres. This integral can be evaluated numerically in prolate spheroidal (PS) coordinates

$$\begin{aligned} x &= a \operatorname{sh} u \sin v \cos \phi, & u &\in (0, \infty), \\ y &= a \operatorname{sh} u \sin v \sin \phi, & v &\in [0, \pi], \\ z &= a \operatorname{csh} u \cos v, & \phi &\in [0, 2\pi]. \end{aligned} \quad (30)$$

The Jacobian of the transformation is

$$\begin{aligned} J &= a^3 (\operatorname{sh}^2 u + \sin^2 v) \operatorname{sh} u \sin v du dv d\phi \\ &= -a^3 g(u, v) du dv d\phi, \quad g(u, v) = (\operatorname{csh}^2 u - v^2) \operatorname{sh} u, \end{aligned} \quad (31)$$

where $v = \cos v$, $v \in [+1, -1]$. The integral in Cartesian coordinates reads in the PS coordinates as

$$\begin{aligned} \int f(x, y, z) dx dy dz &= a^3 \int_0^{2\pi} d\phi \int_0^{\infty} \\ &\times du \int_{-1}^{+1} dv g(u, v) f(u, v, \phi). \end{aligned} \quad (32)$$

The two-centre integral of the type (29) where $\rho^A(|\mathbf{r}|)$ and $V^B(|\mathbf{r} - \mathbf{d}|)$ are two spherical distributions on two different centres reads as

$$I(\mathbf{R}_A, \mathbf{R}_B, \mathbf{T}) = 2\pi a^3 \int_0^{\infty} du \int_{-1}^{+1} dv g(u, v) \rho^A(r_a) V^B(r_b), \quad (33)$$

where r_a and r_b are distances to centres A and B , respectively

$$\begin{aligned} r_a &= a(\operatorname{csh} u + v), \\ r_b &= a(\operatorname{csh} u - v), \quad a = \frac{d}{2}. \end{aligned} \quad (34)$$

Note that integral (33) depends on d —the distance between the two centres. The parameter d enters the integral explicitly through the prefactor a^3 which stems from the Jacobian of the transformation and implicitly through the functional dependence of $\rho^A(r_a)$ and $V^B(r_b)$.

To calculate the derivatives of the pair interaction integral we note that

$$\begin{aligned} \frac{\partial I}{\partial R_A^{\alpha}} &= \frac{\partial I}{\partial d} \frac{\partial d}{\partial R_A^{\alpha}} = \frac{\partial I}{\partial d} \frac{d^{\alpha}}{d} (-1) = -\frac{\partial I}{\partial d} \frac{R_B^{\alpha} + T^{\alpha} - R_A^{\alpha}}{|\mathbf{R}_B + \mathbf{T} - \mathbf{R}_A|}, \\ \frac{\partial I}{\partial R_B^{\alpha}} &= \frac{\partial I}{\partial d} \frac{\partial d}{\partial R_B^{\alpha}} = \frac{\partial I}{\partial d} \frac{d^{\alpha}}{d} = -\frac{\partial I}{\partial R_A^{\alpha}}. \end{aligned} \quad (35)$$

We obtain the following expression for the derivative of the two-centre integral with respect to the distance between the centres

$$\begin{aligned} \frac{\partial I}{\partial d} &= \pi 3a^2 \int_0^{\infty} du \int_{-1}^{+1} dv g(u, v) \rho^A(r_a) V^B(r_b) \\ &+ 2\pi a^3 \int_0^{\infty} du \int_{-1}^{+1} dv g(u, v) \frac{\partial \rho^A(r_a)}{\partial r_a} \frac{\partial r_a}{\partial d} V^B(r_b) \\ &+ 2\pi a^3 \int_0^{\infty} du \int_{-1}^{+1} dv g(u, v) \rho^A(r_a) \frac{\partial r_b}{\partial d} \frac{\partial V^B(r_b)}{\partial r_b} \\ &= \frac{3}{d} I + \frac{2\pi a^3}{d} \int_0^{\infty} du \int_{-1}^{+1} dv g(u, v) \\ &\times \left(r_a \frac{\partial \rho^A(r_a)}{\partial r_a} V^B(r_b) + r_b \rho^A(r_a) \frac{\partial V^B(r_b)}{\partial r_b} \right). \end{aligned} \quad (36)$$

Note that the integrand in the last expression contains the radial derivatives of both atomic density and potential.

6. BAND gradient in the frozen core approximation

This last section briefly sketches an implementation of the BAND energy gradients in the frozen core approximation (FCA) [35, 36]. The details of implementation of gradients in FCA for molecules are given in [4]. The FCA allows one to speed up the SCF procedure by treating only valence electrons variationally. In the FCA, the electrons are divided into ‘core’ and valence and it is assumed that the ‘core’ electrons do not participate in the formation of chemical bonds. Then, as usual, the Bloch basis set functions are constructed. By default, the numerical atomic orbitals (NAOs) from free atomic calculations are used to build up a ‘minimal’ Bloch basis to describe the core electrons, whereas both NAOs and STOs are used to construct a valence Bloch basis set

$$\begin{aligned}\chi_{p\mathbf{k}}^c(\mathbf{r}) &= \sum_{\mathbf{T}} \exp(\mathbf{i}\mathbf{k}\mathbf{T}) \chi_p(\mathbf{r} - \mathbf{R}_p - \mathbf{T}), \quad p \in 1 \dots N_c, \\ \chi_{\mu\mathbf{k}}^v(\mathbf{r}) &= \sum_{\mathbf{T}} \exp(\mathbf{i}\mathbf{k}\mathbf{T}) \chi_{\mu}(\mathbf{r} - \mathbf{R}_{\mu} - \mathbf{T}), \\ &\mu \in 1 \dots N_v^B, \quad N_v^B > N_v,\end{aligned}\quad (37)$$

where N_v^B and N_c is the number of ‘core’ and ‘valence’ electrons. The ‘valence’ Bloch basis set functions are then orthogonalized to the ‘core’ for each \mathbf{k} to obtain a VOC basis set

$$\begin{aligned}\bar{\chi}_{\mathbf{k}}^{\text{voc}} &= (\chi_{1\mathbf{k}}^{\text{voc}}, \dots, \chi_{N_v^B\mathbf{k}}^{\text{voc}}) = \bar{\chi}_{\mathbf{k}}^v - \bar{\chi}_{\mathbf{k}}^c O^{v/\text{voc}}(\mathbf{k}), \\ &= (\chi_{1\mathbf{k}}^v, \dots, \chi_{N_v^B\mathbf{k}}^v) - (\chi_{1\mathbf{k}}^c, \dots, \phi_{N_c\mathbf{k}}^c) O^{v/\text{voc}}(\mathbf{k}),\end{aligned}\quad (38)$$

where $O^{v/\text{voc}}(\mathbf{k}) = (S^{c/c}(\mathbf{k}))^{-1} S^{c/v}(\mathbf{k})$ is the $N_c \times N_v^B$ transformation matrix which ensures that the VOC basis set spans the subspace which is orthogonal to the ‘core’ states. $S^{c/c}(\mathbf{k})$ and $S^{c/v}(\mathbf{k})$ are the overlap matrices between the core–core and core–valence Bloch basis set functions, respectively. The core–valence overlap matrix is defined as

$$S^{c/v}(\mathbf{k}) = \int_{\text{WS}} \bar{\chi}_{\mathbf{k}}^{c\dagger} \bar{\chi}_{\mathbf{k}}^v \, d\mathbf{r}, \quad S^{c/c}(\mathbf{k}) = \int_{\text{WS}} \bar{\chi}_{\mathbf{k}}^{c\dagger} \bar{\chi}_{\mathbf{k}}^c \, d\mathbf{r}, \quad (39)$$

and the other matrices are defined in a similar fashion.

The SCF calculations are then carried out in the VOC basis. Note that a VOC basis set function depends on several ‘centres’, whereas valence (V) or core (C) basis

set functions depend on one centre (one sublattice) only. Therefore, in order to take the derivative, the BAND’s energy has to be written explicitly in terms of the (V)+(C) basis set. For example, the kinetic energy is

$$\begin{aligned}T_s &= \sum_{\mathbf{k} \in \text{IBZ}} \text{Tr}\{P^{\text{voc}}(\mathbf{k}) T^{\text{voc}/\text{voc}}(\mathbf{k})\}, \quad T^{\text{voc}/\text{voc}}(\mathbf{k}) \\ &= \int_{\text{WS}} \bar{\chi}_{\mathbf{k}}^{\text{voc}\dagger} \left(-\frac{1}{2} \nabla^2\right) \bar{\chi}_{\mathbf{k}}^{\text{voc}} \, d\mathbf{r}, \\ T^{\text{voc}/\text{voc}}(\mathbf{k}) &= T^{v/v}(\mathbf{k}) - O^{v/\text{voc}\dagger}(\mathbf{k}) T^{c/v}(\mathbf{k}) - T^{v/c}(\mathbf{k}) O^{v/\text{voc}}(\mathbf{k}) \\ &\quad + O^{v/\text{voc}\dagger}(\mathbf{k}) T^{c/c}(\mathbf{k}) O^{v/\text{voc}}(\mathbf{k}),\end{aligned}\quad (40)$$

where \mathbf{P}^{voc} is the \mathbf{P} -matrix in the VOC basis set and the VOC overlap matrix is

$$\begin{aligned}S^{\text{voc}/\text{voc}}(\mathbf{k}) &= \int_{\text{WS}} \bar{\chi}_{\mathbf{k}}^{\text{voc}\dagger} \bar{\chi}_{\mathbf{k}}^{\text{voc}} \, d\mathbf{r} = S^{v/v}(\mathbf{k}) \\ &\quad - O^{v/\text{voc}\dagger}(\mathbf{k}) S^{c/v}(\mathbf{k}) - S^{v/c}(\mathbf{k}) O^{v/\text{voc}}(\mathbf{k}) \\ &\quad + O^{v/\text{voc}\dagger}(\mathbf{k}) S^{c/c}(\mathbf{k}) O^{v/\text{voc}}(\mathbf{k}).\end{aligned}\quad (41)$$

The total energy E can be written as an explicit function of the \mathbf{P} -matrix in the VOC basis set— \mathbf{P}^{voc} , the transformation matrix $\mathbf{O}^{v/\text{voc}}$, and the (V) + (C) basis set functions. Differentiating the total energy, we obtain

$$\begin{aligned}\frac{dE}{dR_B^y} &= \sum_{\mathbf{k}} \sum_{\mu\nu}^{N_v^B} \frac{\partial E}{\partial P_{\mu\nu}^{\text{voc}}(\mathbf{k})} \frac{\partial P_{\mu\nu}^{\text{voc}}(\mathbf{k})}{\partial R_B^y} + \sum_{\mathbf{k}} \sum_{\mu\nu}^{N_v^B} \\ &\quad \times \frac{\partial E}{\partial P_{\mu\nu}^{\text{voc}}(\mathbf{k})} \sum_{p\delta}^{(N_c, N_v^B)} \frac{\partial P_{\mu\nu}^{\text{voc}}(\mathbf{k})}{\partial O_{p\delta}^{v/\text{voc}}(\mathbf{k})} \frac{\partial O_{p\delta}^{v/\text{voc}}(\mathbf{k})}{\partial R_B^y} \\ &\quad + \frac{\partial E}{\partial R_B^y} + \sum_{\mathbf{k}} \sum_{\mu}^{N_v^B} \sum_p^{N_c} \frac{\partial E}{\partial O_{p\mu}^{v/\text{voc}}(\mathbf{k})} \frac{\partial O_{p\mu}^{v/\text{voc}}(\mathbf{k})}{\partial R_B^y}.\end{aligned}\quad (42)$$

The first two terms in (42) look formidable but they can be combined together to give a familiar energy-weighted \mathbf{P}^e -matrix term

$$\begin{aligned}- \sum_{\mathbf{k}} \sum_{\mu\nu}^{N_v^B} P_{\mu\nu}^{\text{voc},e}(\mathbf{k}) &\left(\frac{\partial S_{\mu\nu}^{v/v}(\mathbf{k})}{\partial R_B^y} - \sum_{\alpha} \frac{\partial S_{\mu\alpha}^{v/c}(\mathbf{k})}{\partial R_B^y} O_{\alpha\nu}^{v/\text{voc}}(\mathbf{k}) \right. \\ &\quad \left. - \sum_{\alpha} O_{\mu\alpha}^{v/\text{voc}\dagger}(\mathbf{k}) \frac{\partial S_{\alpha\nu}^{c/v}(\mathbf{k})}{\partial R_B^y} \right).\end{aligned}\quad (43)$$

In deriving (43) we assumed $\partial(S^{c/c}(\mathbf{k}))^{-1}/\partial R_B^y = 0$.

To obtain the third term $\partial E/\partial R_B^y$ in (42), we differentiate basis set functions and atomic terms

keeping the \mathbf{P} and $\mathbf{O}^{\text{v/voc}}$ matrices fixed, and to obtain the fourth term we differentiate the energy expression with respect to $\mathbf{O}^{\text{v/voc}}$ matrix elements keeping everything else fixed. The last two terms in (42) can be combined to obtain the final expression for the energy gradient in the FCA which strongly resembles (6). The energy-weighted \mathbf{P}^e -matrix term in the FCA case is given by (43). The kinetic energy contribution to the gradient $\partial T_s / \partial R_B^\gamma$ can be derived straightforwardly from (40). Finally, the xc and Coulomb contribution to the analytic energy gradient in the FCA have the same form as in the all-electron case (6). The construction of the density gradient requires modification as the density is expressed now in terms of the (V) + (C) basis.

The procedure outlined in section 4 is referred to as the construction of the density gradients via the \mathbf{P} -matrix route. In the case of the FCA, the \mathbf{P} -matrix route would involve differentiating expressions involving complicated products of matrices and basis set functions which, in turn, entails a complicated loop structure. Therefore, it is more expedient in this case to adopt the so-called ‘band-by-band’ construction procedure. In the ‘band-by-band’ procedure we explicitly construct the gradient of all the bands and the density gradient is obtained by summing over the bands

$$\begin{aligned} \frac{\partial \rho_\sigma^{\text{irr}}(\mathbf{k}, \mathbf{r})}{\partial R_B^\gamma} &= \sum_{\epsilon_{\mathbf{k}}^\sigma < E_f} 2n_i^\sigma(\mathbf{k}) \operatorname{Re} \left\{ \psi_{\mathbf{k}}^{\sigma\dagger}(\mathbf{r}) \frac{\partial \psi_{\mathbf{k}}^\sigma(\mathbf{r})}{\partial R_B^\gamma} \right\}, \quad \mathbf{r} \in \text{WS}, \\ \frac{\partial \psi_{\mathbf{k}}^\sigma}{\partial R_B^\gamma} &= \sum_{m=1}^{N_v^\sigma} c_{mi}^\sigma(\mathbf{k}) \left[\frac{\partial \chi_{m\mathbf{k}}^\sigma}{\partial R_B^\gamma} - \sum_{\delta=1}^{N_c} \right. \\ &\quad \left. \times \left(\frac{\partial O_{\delta m}^{\text{v/voc}}(\mathbf{k})}{\partial R_B^\gamma} \chi_{\delta\mathbf{k}}^c + O_{\delta m}^{\text{v/voc}}(\mathbf{k}) \frac{\partial \chi_{\delta\mathbf{k}}^c}{\partial R_B^\gamma} \right) \right]. \end{aligned} \quad (44)$$

The symmetrization of all gradient terms in the FCA follows the same path as in the all-electron case.

7. Examples from numerical tests

Our implementation was subjected to a number of tests.

One of the simplest conceivable tests of analytic gradients in solid state codes is the molecular optimization in the supercell geometry. We performed a series of calculations on the CO molecule which was placed in a large cubic supercell with $a = 20 \text{ \AA}$. The oxygen was put at the origin $(0, 0, 0)$, whereas the carbon atom was placed at some distance along the positive z axis at position $(0, 0, d)$. We performed a series of LDA calculations by varying the z coordinate of the carbon atom. The all-electron TZ2P STO/NAO basis set from

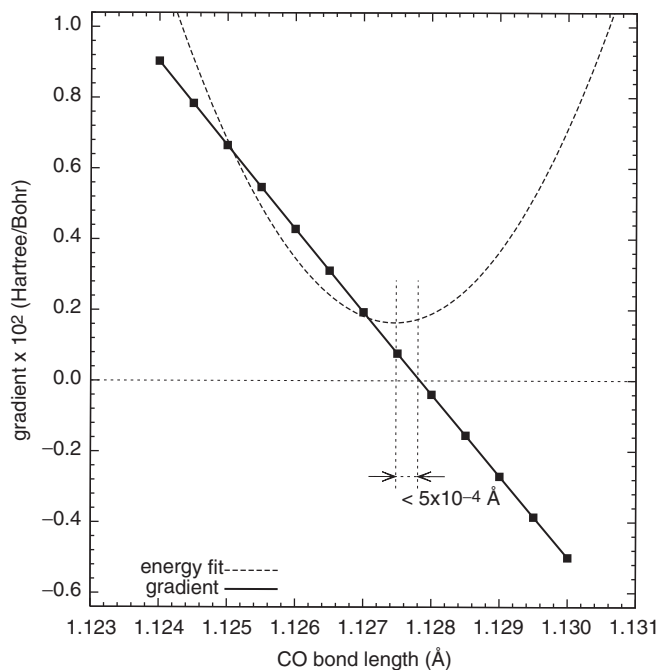


Figure 1. Energy gradient of CO molecule and energy profile as a function of diatomic distance d between carbon and oxygen. LDA/TZ2P calculation with Accuracy = 5, no dispersion, and large supercell. In the energy profile, the energy is in arbitrary units with arbitrary chosen zero point energy. The profile is constructed by fitting energy values to the parabola with least-squares fit. The agreement in the equilibrium bond length as deduced from the energy gradient and energy profile is better than $5 \times 10^{-4} \text{ \AA}$.

BAND’s basis set database was employed, dispersion was neglected, and the general accuracy parameter which, for example, controls the precision of numerical integration was set up relatively high (Accuracy = 5). Figure 1 shows the analytic force $-dE/dR_C^z$ acting on the carbon atom in the z direction as a function of d together with the ‘bond length energy profile’ obtained by a least-squares fit. From the energy profile it follows that the energy minimum is attained for $d \approx 1.127 - 1.128 \text{ \AA}$. The experimental bond length is 1.128 \AA [38]. In agreement with the energy profile, for bond lengths which are smaller than the equilibrium bond length, the force acting on the carbon atom is positive and decreases as the bond length increases. The force passes through zero between $1.127 - 1.128 \text{ \AA}$ and becomes negative for larger bond lengths. Overall, the sign and magnitude of the force is consistent with the energy profile. As can be seen from figure 1, the discrepancy between the equilibrium bond length deduced from the analytic gradient and energy profile is less than 0.0005 \AA .

Figures 2 and 3 compare the analytic force from our implementation and the force obtained by numerical

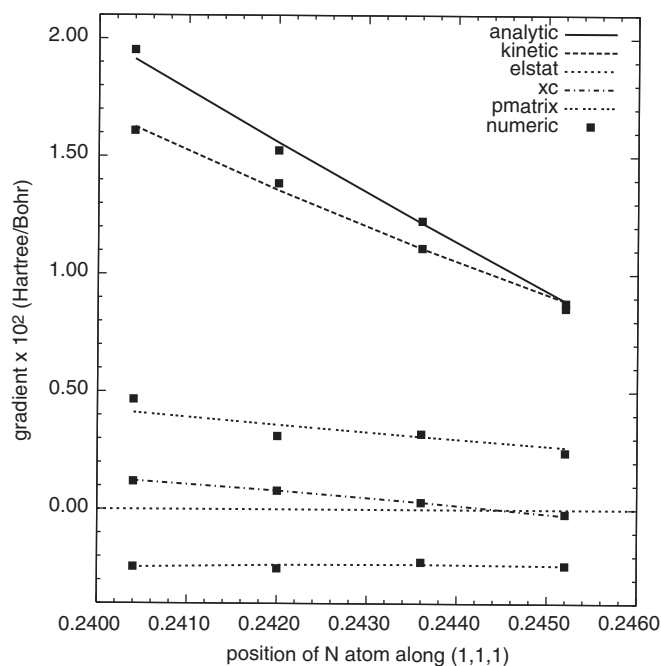


Figure 2. Contributions to the analytic force acting on the nitrogen atom in BN crystal as a function of the B–N distance. Only one component of the force is shown. The B atom is located at the origin and fixed; N is located on and moved along the cube’s diagonal (1,1,1). The lattice constant is $a=3.616\text{ \AA}$ and the distance between the atoms is $3^{1/2} * a \times$ fractional coordinate. The fractional coordinate of 0.25 for the nitrogen atom corresponds to the zincblende structure at which the analytic force is zero (not shown). LDA/TZ2P calculation with Accuracy=5 and dispersion. The total force is partitioned into various contributions: kinetic–kinetic energy contribution; elstat–electrostatic energy contribution; xc–xc energy contribution; pmatrix–energy-weighted \mathbf{P}^e -matrix contribution. The analytic force is compared to the one obtained using numerical differentiation as described in the text.

differentiation of energy terms in the boron nitride and silicon solids for a number of interatomic (B–N and Si–Si) distances. Note that the calculations for the silicon were carried out in the frozen core approximation. In both calculations, one of the atoms was fixed at the origin (B and Si), whereas the other atom (N and Si) was moved away from the first along the direction (1,1,1) (along the cube’s diagonal). For each of the interatomic distances, we have calculated the force acting on the atoms located on the cube’s diagonal (N and Si) and also various contributions to the force both analytically and numerically. The numerical partial derivatives of the energy terms were determined using a five-point central difference scheme under the condition that the MO coefficients were kept fixed. The numerical energy-weighted \mathbf{P}^e -matrix contribution was obtained as the difference between the total and partial energy derivatives. Figures 2 and 3 confirm that our

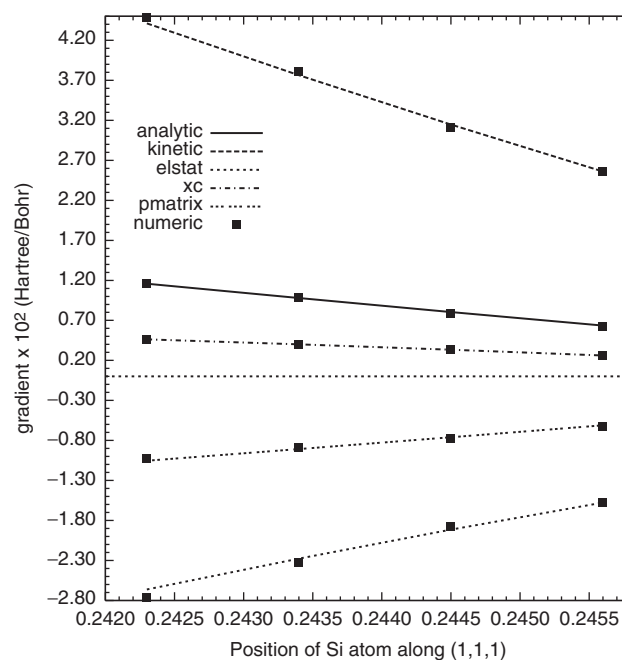


Figure 3. Contributions to the analytic force acting on the silicon atom in Si crystal as a function of the Si–Si distance. Only one component of the force is shown. One of the Si atoms is located at the origin and fixed; the other Si atom is located on and moved along the cube’s diagonal (1,1,1). The lattice constant is $a=5.43\text{ \AA}$ and the distance between the atoms is $3^{1/2} * a \times$ fractional coordinate. The fractional coordinate of 0.25 corresponds to the diamond structure at which the analytic force is zero (not shown). Frozen core LDA/TZ2P calculation with Accuracy=5 and dispersion. The total force is partitioned into various contributions: kinetic–kinetic energy contribution; elstat–electrostatic energy contribution; xc–xc energy contribution; pmatrix–energy-weighted \mathbf{P}^e -matrix contribution. The analytic force is compared to the one obtained using numerical differentiation as described in the text.

implementation in the all-electron and frozen core approximation cases is indeed correct and yields analytic energy gradients which are the total derivatives of the energy. The discrepancy between the analytic and numerical forces is less than 0.0004 (H/B) and the total energy derivative can be more accurate than the individual terms due to an error cancellation. Overall, we have a good agreement between the forces obtained analytically and through the numerical differentiation.

8. Concluding remarks

The analytic energy gradients with respect to atomic coordinates are implemented in the BAND program for periodic calculations based on the KS DFT formulation. Our implementation differs from others in the direct use of a Bloch basis set made up of Slater-type and numeric

atomic orbitals and does not hinge upon the particular nature of AOs—other types of AOs can be easily implemented. The details of our implementation are described including the use of symmetry in the reciprocal and direct spaces, as well as the application of the frozen core approximation. Integration in the reciprocal space is carried out on the irreducible Brillouin zone and the symmetry operations are applied to obtain the integrals

$$\begin{aligned}
\{\mathbf{o}; \mathbf{t}_o\} \chi_{v_B}^{\mathbf{k}}(\mathbf{r}) &= \sum_{\mathbf{T}} \exp(i\mathbf{k} \cdot \mathbf{T}) \{\mathbf{o}; \mathbf{t}_o\} \chi_{v_B}(\mathbf{r} - \mathbf{R}_B - \mathbf{T}) \\
&= \sum_{\mathbf{T}} \exp(i\mathbf{o}\mathbf{k} \cdot \mathbf{o}\mathbf{T}) \chi_{v_B}(\mathbf{o}^{-1}(\mathbf{r} - \mathbf{t}_o - \mathbf{o} \cdot \mathbf{R}_B - \mathbf{o} \cdot \mathbf{T})) \\
&= \sum_{\mathbf{T}} \exp(i\mathbf{o}\mathbf{k} \cdot (\mathbf{o}\mathbf{T} + \mathbf{T}_B(\alpha))) \chi_{v_B}(\mathbf{o}^{-1}(\mathbf{r} - \mathbf{R}_{(\hat{o}B)} - (\mathbf{o}\mathbf{T} + \mathbf{T}_B(\mathbf{o})))) \exp(-i\mathbf{o}\mathbf{k} \cdot \mathbf{T}_B(\mathbf{o})) \\
&= \exp(-i\mathbf{o}\mathbf{k} \cdot \mathbf{T}_B(\mathbf{o})) \sum_{\mathbf{T}} \exp(i\mathbf{o}\mathbf{k} \cdot \mathbf{T}) \chi_{v_B}(\mathbf{o}^{-1}(\mathbf{r} - \mathbf{R}_{(\hat{o}B)} - \mathbf{T})), \tag{A4}
\end{aligned}$$

over the whole Brillouin zone. Symmetry in the direct space is used to speed up the calculations and decrease the memory requirements. Special care is taken to ensure that the numerical errors are minimized. The analytic gradients are also implemented in the frozen core approximation in which only the valence electrons are treated variationally and, hence, the computational cost of the SCF procedure is reduced.

EK acknowledges financial support from the Alberta Ingenuity Fund and stimulating discussions with Dr P. H. T. Philipsen.

Appendix A: Integration in the reciprocal space using IBZ

The rotated Bloch state with wavevector \mathbf{k} translates as Bloch state with wavevector $\mathbf{o}\mathbf{k}$

$$\begin{aligned}
\{\mathbf{e}; \mathbf{T}\} \{\mathbf{o}; \mathbf{t}_o\} |\psi_i^{\mathbf{k}}\rangle &= \{\mathbf{o}; \mathbf{t}_o\} \{\mathbf{e}; \mathbf{o}^{-1}\mathbf{T}\} |\psi_i^{\mathbf{k}}\rangle \\
&= \exp(-i\mathbf{o}\mathbf{k} \cdot \mathbf{T}) \{\mathbf{o}; \mathbf{t}_o\} |\psi_i^{\mathbf{k}}\rangle, \tag{A1}
\end{aligned}$$

and $\psi_i^{\mathbf{o}\mathbf{k}}$ can be expanded as a linear combination of rotated in real space one-electron states at \mathbf{k} . The sum is over all one-electron states degenerate to $\varepsilon_i^{\mathbf{k}}$

$$\begin{aligned}
\psi_i^{\mathbf{o}\mathbf{k}}(\mathbf{r}) &= \sum_{\varepsilon_j^{\mathbf{k}}=\varepsilon_i^{\mathbf{k}}} d_{ji}^{\mathbf{k}}(\mathbf{o}) \{\mathbf{o}; \mathbf{t}_o\} \psi_j^{\mathbf{k}}(\mathbf{r}) \\
&= \sum_{\varepsilon_j^{\mathbf{k}}=\varepsilon_i^{\mathbf{k}}} d_{ji}^{\mathbf{k}}(\mathbf{o}) \sum_B \sum_{v_B} c_{v_B j}^{\mathbf{k}} \{\mathbf{o}; \mathbf{t}_o\} \chi_{v_B}^{\mathbf{k}}(\mathbf{r}). \tag{A2}
\end{aligned}$$

In the last equation, we expanded the one-electron states in terms of Bloch basis set functions which are

linear combinations of lattice translated AOs centred at \mathbf{R}_B

$$\chi_{v_B}^{\mathbf{k}}(\mathbf{r}) = \sum_{\mathbf{T}} \exp(i\mathbf{k} \cdot \mathbf{T}) \chi_{v_B}(\mathbf{r} - \mathbf{R}_B - \mathbf{T}). \tag{A3}$$

Under a rotation, the Bloch basis set function transforms as

where we introduced notation for an atom centred at $\mathbf{R}_{(\hat{o}B)} + \mathbf{T}_B(\mathbf{o}) = \mathbf{o} \cdot \mathbf{R}_B + \mathbf{t}_o$. We then can expand rotated atomic orbitals centred at $\mathbf{R}_{(\hat{o}B)}$ as

$$\begin{aligned}
\chi_{v_B}(\mathbf{o}^{-1}(\mathbf{r} - \mathbf{R}_{(\hat{o}B)} - \mathbf{T})) \\
= \sum_{\mu_{(\hat{o}B)}} D_{\mu_{(\hat{o}B)} v_B}(\mathbf{o}) \chi_{\mu_{(\hat{o}B)}}(\mathbf{r} - \mathbf{R}_{(\hat{o}B)} - \mathbf{T}) \tag{A5}
\end{aligned}$$

and obtain expression for the rotated Bloch basis set function at \mathbf{k}

$$\{\mathbf{o}; \mathbf{t}_o\} \chi_{v_B}^{\mathbf{k}}(\mathbf{r}) = \exp(-i\mathbf{o}\mathbf{k} \cdot \mathbf{T}_B(\mathbf{o})) \sum_{\mu_{(\hat{o}B)}} D_{\mu_{(\hat{o}B)} v_B}(\mathbf{o}) \chi_{\mu_{(\hat{o}B)}}^{\mathbf{o}\mathbf{k}}(\mathbf{r}). \tag{A6}$$

Using the expression for the rotated Bloch basis set functions, we obtain the following equation with respect to the expansion coefficients $\{c_{\mu_{Ai}}^{\mathbf{k}}\}$

$$\begin{aligned}
\sum_A \sum_{\mu_A} c_{\mu_A i}^{\mathbf{o}\mathbf{k}} \chi_{\mu_A}^{\mathbf{o}\mathbf{k}}(\mathbf{r}) &= \sum_{\varepsilon_j^{\mathbf{k}}=\varepsilon_i^{\mathbf{k}}} \sum_B \sum_{v_B} d_{ji}^{\mathbf{k}}(\mathbf{o}) c_{v_B j}^{\mathbf{k}} \exp(-i\mathbf{o}\mathbf{k} \cdot \mathbf{T}_B(\mathbf{o})) \\
&\quad \times \sum_{\mu_{(\hat{o}B)}} D_{\mu_{(\hat{o}B)} v_B}(\mathbf{o}) \chi_{\mu_{(\hat{o}B)}}^{\mathbf{o}\mathbf{k}}(\mathbf{r}). \tag{A7}
\end{aligned}$$

Introducing the notation $A' = \hat{o}^{-1}A$, we obtain

$$\begin{aligned}
c_{\mu_{Ai}}^{\mathbf{o}\mathbf{k}} &= \exp(-i\mathbf{o}\mathbf{k} \cdot \mathbf{T}_{A'}(\mathbf{o})) \sum_{\varepsilon_j^{\mathbf{k}}=\varepsilon_i^{\mathbf{k}}} d_{ji}^{\mathbf{k}}(\mathbf{o}) \sum_{\mu_{A'}} c_{\mu_{A'} j}^{\mathbf{k}} D_{\mu_{A'} \mu_{A'}}(\mathbf{o}), \\
c_{v_B i}^{\mathbf{o}\mathbf{k}} &= \exp(-i\mathbf{o}\mathbf{k} \cdot \mathbf{T}_{B'}(\mathbf{o})) \sum_{\varepsilon_j^{\mathbf{k}}=\varepsilon_i^{\mathbf{k}}} d_{ji}^{\mathbf{k}}(\mathbf{o}) \sum_{v_{B'}} c_{v_{B'} j}^{\mathbf{k}} D_{v_{B'} v_{B'}}(\mathbf{o}). \tag{A8}
\end{aligned}$$

Finally, we obtain the following expression for the \mathbf{P} -matrix at $\mathbf{o}\mathbf{k}$

$$\begin{aligned}
P_{\mu_{AVB}}^{\mathbf{o}\mathbf{k}} &= \sum_i c_{\mu_{A'} i}^{\mathbf{o}\mathbf{k} \dagger} c_{v_B i}^{\mathbf{o}\mathbf{k}} = \exp(i\mathbf{o}\mathbf{k} \cdot (\mathbf{T}_{A'}(\mathbf{o}) - \mathbf{T}_{B'}(\mathbf{o}))) \\
&\quad \times \sum_{\mu_{A'} v_{B'}} P_{\mu_{A'} v_{B'}}^{\mathbf{k}} D_{\mu_{A'} \mu_{A'}}^{\dagger} D_{v_{B'} v_{B'}} \tag{A9}
\end{aligned}$$

Employing the symmetry in the reciprocal space, an expectation value of an operator \hat{A} writes

$$\langle \hat{A} \rangle = \frac{1}{N_{\hat{o}}} \sum_{\hat{o}} \sum_{\mathbf{k} \in \text{IBZ}} \sum_{AB} \sum_{\mu_A \nu_B} P_{\mu_A \nu_B}^{\text{ok}} \langle \chi_{\mu_A}^{\text{ok}} | \hat{A} | \chi_{\nu_B}^{\text{ok}} \rangle, \quad (\text{A10})$$

where the \mathbf{k} -space integration weights satisfy $\sum_{\mathbf{k} \in \text{IBZ}} w(\mathbf{k}) = 1$. Substituting the expression for the \mathbf{P} -matrix at ok in terms of the \mathbf{P} -matrix at \mathbf{k} in (A10) and employing (A6), we obtain

$$\langle \hat{A} \rangle = \frac{1}{N_{\hat{o}}} \sum_{\hat{o}} \sum_{\mathbf{k} \in \text{IBZ}} \sum_{AB} \sum_{\mu_A \nu_B} P_{\mu_A \nu_B}^{\mathbf{k}} \langle \{\mathbf{o}; \mathbf{t}_o\} \chi_{\mu_A}^{\mathbf{k}} | \hat{A} | \{\mathbf{o}; \mathbf{t}_o\} \chi_{\nu_B}^{\mathbf{k}} \rangle. \quad (\text{A11})$$

Appendix B: A1-symmetry of the deformation density

We first show that the ‘atomic’ density ρ_e is A1-symmetric and then that the SCF density is A1-symmetric. The deformation density $\Delta\rho$ is A1-symmetric as the difference of two A1-symmetric quantities. The electron atomic density is

$$\rho_e(\mathbf{r}) = \sum_A \rho_e^A, \quad \rho_e^A = \sum_{\mathbf{T}} \rho_e^A(|\mathbf{r} - \mathbf{R}_A - \mathbf{T}|). \quad (\text{B1})$$

We then apply symmetry operation $\{\mathbf{o}; \mathbf{t}_o\}$ to ρ_e and obtain

$$\begin{aligned} \{\mathbf{o}; \mathbf{t}_o\} \rho_e(\mathbf{r}) &= \sum_A \sum_{\mathbf{T}} \{\mathbf{o}; \mathbf{t}_o\} \rho_e^A(|\mathbf{r} - \mathbf{R}_A - \mathbf{T}|) \\ &= \sum_A \sum_{\mathbf{T}} \rho_e^A(|\mathbf{o}^{-1} \cdot (\mathbf{r} - \mathbf{R}_{(\hat{o}A)} - \mathbf{o} \cdot \mathbf{T} - \mathbf{T}_A(\mathbf{o}))|). \end{aligned} \quad (\text{B2})$$

The rotation will not change the value of $\rho_e^A(|\mathbf{r}|)$ as it is spherically symmetric, therefore,

$$\begin{aligned} \rho_e^A(|\mathbf{o}^{-1} \cdot (\mathbf{r} - \mathbf{R}_{(\hat{o}A)} - \mathbf{o} \cdot \mathbf{T} - \mathbf{T}_A(\mathbf{o}))|) \\ = \rho_e^A(|\mathbf{r} - \mathbf{R}_{(\hat{o}A)} - \mathbf{o} \cdot \mathbf{T} - \mathbf{T}_A(\mathbf{o})|) \end{aligned} \quad (\text{B3})$$

$$\begin{aligned} \{\alpha; t_\alpha\} \tilde{\rho}^C(\mathbf{r}) &= \frac{1}{N_{\hat{o}}} \sum_{\hat{o}} \sum_{\mathbf{k} \in \text{IBZ}} \left[\sum_{\mu_C \nu_C} P_{\mu_C \nu_C}^{\text{ok}} \{\alpha; t_\alpha\} \chi_{\mu_C}^{\text{ok}\dagger}(\mathbf{r}) + \{\alpha; t_\alpha\} \chi_{\nu_C}^{\text{ok}}(\mathbf{r}) + \sum_B \sum_{\mu_C \nu_B} 2 \text{Re} \left\{ P_{\mu_C \nu_B}^{\text{ok}} \{\alpha; t_\alpha\} \chi_{\mu_C}^{\text{ok}\dagger}(\mathbf{r}) \{\alpha; t_\alpha\} \chi_{\nu_B}^{\text{ok}}(\mathbf{r}) \right\} \right] \\ &= \frac{1}{N_{\hat{o}}} \sum_{\hat{o}} \sum_{\mathbf{k} \in \text{IBZ}} \left[\sum_{\mu'(\hat{o}C) \nu'(\hat{o}C)} P_{\mu'(\hat{o}C) \nu'(\hat{o}C)}^{\gamma\mathbf{k}} \{\alpha; t_\alpha\} \chi_{\mu'(\hat{o}C)}^{\gamma\mathbf{k}\dagger}(\mathbf{r}) \right. \\ &\quad \left. + \{\alpha; t_\alpha\} \chi_{\nu'(\hat{o}C)}^{\gamma\mathbf{k}}(\mathbf{r}) + \sum_B \sum_{\mu'(\hat{o}C) \nu'(\hat{o}B)} 2 \text{Re} \left\{ P_{\mu'(\hat{o}C) \nu'(\hat{o}B)}^{\gamma\mathbf{k}} \{\alpha; t_\alpha\} \chi_{\mu'(\hat{o}C)}^{\gamma\mathbf{k}\dagger}(\mathbf{r}) \{\alpha; t_\alpha\} \chi_{\nu'(\hat{o}B)}^{\gamma\mathbf{k}}(\mathbf{r}) \right\} \right] \\ &= \tilde{\rho}^{(\hat{o}C)}(\mathbf{r}). \end{aligned} \quad (\text{B9})$$

and

$$\{\mathbf{o}, t_o\} \rho_e(\mathbf{r}) = \sum_A \sum_{\mathbf{T}} \rho_e^{\text{ok}A}(|\mathbf{r} - \mathbf{R}_{\text{ok}A} - \mathbf{T}'|) = \sum_A \rho_e^{\text{ok}A} = \rho_e(\mathbf{r}), \quad (\text{B4})$$

which proves that the sum of the spherically symmetric atomic densities is an A1-symmetric quantity.

The proof that the SCF density is A1-symmetric is a little bit more involved and requires the application of some of the equations derived in Appendix A. The SCF density is

$$\rho(\mathbf{r}) = \frac{1}{N_{\hat{o}}} \sum_{\hat{o}} \sum_{\mathbf{k} \in \text{IBZ}} \sum_{AB} \sum_{\mu_A \nu_B} P_{\mu_A \nu_B}^{\text{ok}} \chi_{\mu_A}^{\text{ok}\dagger}(\mathbf{r}) \chi_{\nu_B}^{\text{ok}}(\mathbf{r}). \quad (\text{B5})$$

Applying a symmetry operation $\{\alpha; t_\alpha\}$ to the density, we obtain

$$\begin{aligned} \{\alpha; t_\alpha\} \rho(\mathbf{r}) &= \frac{1}{N_{\hat{o}}} \sum_{\hat{o}} \sum_{\mathbf{k} \in \text{IBZ}} \sum_{AB} \sum_{\mu_A \nu_B} P_{\mu_A \nu_B}^{\alpha^{-1}\gamma\mathbf{k}} \\ &\quad \times \{\alpha; t_\alpha\} \chi_{\mu_A}^{\text{ok}\dagger}(\mathbf{r}) \{\alpha; t_\alpha\} \chi_{\nu_B}^{\text{ok}}(\mathbf{r}), \end{aligned} \quad (\text{B6})$$

where we have introduced a notation $\gamma = \alpha \cdot \mathbf{o}$. Taking into account that the rotated basis set function at ok transforms as

$$\{\alpha; t_\alpha\} \chi_{\nu_B'}^{\text{ok}}(\mathbf{r}) = \exp(-i\gamma\mathbf{k} \cdot \mathbf{T}_B'(\alpha)) \sum_{\nu_B} D_{\nu_B' \nu_B}(\alpha) \chi_{\nu_B}^{\gamma\mathbf{k}\dagger}(\mathbf{r}), \quad (\text{B7})$$

we obtain

$$\begin{aligned} \{\alpha; t_\alpha\} \rho(\mathbf{r}) &= \frac{1}{N_{\hat{o}}} \sum_{\hat{o}} \sum_{\mathbf{k} \in \text{IBZ}} \sum_{A'B'} \sum_{\mu_A' \nu_B'} P_{\mu_A' \nu_B'}^{\alpha^{-1}\gamma\mathbf{k}} \\ &\quad \times \exp(i\gamma\mathbf{k} \cdot (\mathbf{T}_A'(\alpha) - \mathbf{T}_B'(\alpha))) \\ &\quad \times \sum_{\mu_A' \nu_B'} D_{\mu_A' \mu_A'}^\dagger(\alpha) D_{\nu_B' \nu_B'}(\alpha) \chi_{\mu_A'}^{\gamma\mathbf{k}\dagger}(\mathbf{r}) \chi_{\nu_B'}^{\gamma\mathbf{k}}(\mathbf{r}) \\ &= \frac{1}{N_{\hat{o}}} \sum_{\hat{o}} \sum_{\mathbf{k} \in \text{IBZ}} \sum_{A'B'} \sum_{\mu_A' \nu_B'} P_{\mu_A' \nu_B'}^{\gamma\mathbf{k}} \chi_{\mu_A'}^{\gamma\mathbf{k}\dagger}(\mathbf{r}) \chi_{\nu_B'}^{\gamma\mathbf{k}}(\mathbf{r}) \\ &= \rho(\mathbf{r}). \end{aligned} \quad (\text{B8})$$

In a similar fashion, it is possible to show that a chunk of the SCF density which explicitly depends on an atom’s coordinate $\tilde{\rho}^C(\mathbf{r})$ transforms as

References

- [1] W. Kohn and L. J. Sham, Phys. Rev. A **140**, 1133 (1965).
[2] P. P. Hohenberg and W. Kohn, Phys. Rev. B **136**, 864 (1964).
[3] L. Versluis and T. Ziegler, J. Chem. Phys. **88**, 322 (1988).
[4] L. Versluis, *PhD thesis, University of Calgary* (Calgary, 1989).
[5] C. Satoko, Chem. Phys. Lett. **83**, 111 (1981).
[6] C. Satoko, Phys. Rev. B **30**, 1754 (1984).
[7] J. Harris, R. O. Jones, and J. E. Müller, J. Chem. Phys. **75**, 3904 (1981).
[8] P. Bendt and A. Zunger, Phys. Rev. Lett. **50**, 1684 (1983).
[9] F. W. Averill and G. S. Painter, Phys. Rev. B **32**, 2141 (1985).
[10] L. Fan and T. Ziegler, J. Chem. Phys. **95**, 7401 (1991).
[11] L. Fan and T. Ziegler, J. Am. Chem. **114**, 10890 (1992).
[12] R. P. Feynman, Phys. Rev. **56**, 340 (1939).
[13] J. Hellmann, *Einführung in die Quantenchemie* (Deuticke and Co., Leipzig, 1937).
[14] P. Pulay, Molec. Phys. **17**, 197 (1969).
[15] M. C. Payne, M. P. Teter, D. C. Allan, T. A. Arias, and J. D. Joannopoulos, Rev. Mod. Phys. **64**, 1045 (1992).
[16] N. A. Modine, G. Zumbach, and E. Kaxiras, Phys. Rev. B **55**, 10289 (1997).
[17] S. Goedecker, Rev. Mod. Phys. **71**, 1085 (1999).
[18] T. L. Beck, Rev. Mod. Phys. **72**, 1041 (2000).
[19] J. VandeVondele, M. Krack, F. Mohamed, M. Parrinello, T. Chassaing, and J. Hutter, Comp. Phys. Commun. **167**, 103 (2005).
[20] D. R. Hamann, M. Schlüter, and C. Chiang, Phys. Rev. Lett. **43**, 1494 (1979).
[21] G. B. Bachelet, D. R. Hamann, and M. Schlüter, Phys. Rev. B **26**, 4199 (1982).
[22] N. Troullier and J. L. Martins, Phys. Rev. B **43**, 1993 (1991).
[23] S. Goedecker, M. Teter, and J. Hutter, Phys. Rev. B **54**, 1703 (1996).
[24] S. Hirata and S. Iwata, J. Phys. Chem. A **102**, 8426 (1998).
[25] M. Tobita, S. Hirata, and R. J. Bartlett, J. Chem. Phys. **118**, 5776 (2003).
[26] K. N. Kudin and G. E. Scuseria, Phys. Rev. B **61**, 16440 (2000).
[27] K. Doll, V. R. Saunders, and N. M. Harrison, Int. J. Quantum Chem. **82**, 1 (2001).
[28] G. te Velde and E. J. Baerends, Phys. Rev. B **44**, 7888 (1991).
[29] P. M. Boerrigter, G. te Velde, and E. J. Baerends, Int. J. Quantum Chem. **33**, 87 (1988).
[30] G. te Velde, *PhD thesis* (Vrije Universiteit, Amsterdam, 1990).
[31] G. Wiesenekker and E. J. Baerends, J. Phys.: Condens. Matt. **3**, 6721 (1991).
[32] G. Wiesenekker, G. te Velde, and E. J. Baerends, J. Phys.: Condens. Matt. **21**, 4263 (1988).
[33] J. P. Perdew and S. Kurth, in *Lecture Notes in Physics*, edited by C. Fiolhais, F. Nogueira, and M.A.L. Marques (Springer-Verlag, Berlin, 2003), Vol. 620, pp. 1–55.
[34] E. J. Baerends, D. E. Ellis, and P. Ros, Chem. Phys. **2**, 41 (1973).
[35] G. te Velde, F. M. Bickelhaupt, E. J. Baerends, C. F. Guerra, S. J. A. van Gisbergen, J. G. Snijders, and T. Ziegler, J. Comp. Chem. **22**, 931 (2001).
[36] U. von Barth and C. D. Gelatt, Phys. Rev. B **21**, 2222 (1980).
[37] S. Flodmark, J. Comput. Phys. **25**, 314 (1977).
[38] K. P. Huber and G. Herzberg, *Molecular Spectra and Molecular Structure. IV. Constants of Diatomic Molecules* (Van Nostrand Reinhold Co, New York, 1979).